A R C H I V E S O F M E T A L L U R G Y A N D M A T E R I A L S
Volume 53 2008 Issue 2

O. J. P. GONZÁLEZ*, Y. I. C. GUZMÁN*, M. A. RAMÍREZ-ARGAEZ**, A. N. CONEJO*

MELTING BEHAVIOR OF SIMULATED DRI IN LIQUID STEEL

SYMULACJA ZJAWISKA TOPNIENIA DRI W CIEKŁEJ STALI

The melting process of sponge iron in electric arc furnaces involves highly complex phenomena of fluid flow, heat and mass transfer in unsteady state conditions. Few attempts worldwide have been carried out to couple these phenomena to describe the melting kinetics. In this work, some preliminary results are presented coupling three models; an arc model for AC electric arcs, a bath model and a melting model. The results describe the influence of some process variables on the melting kinetics of solid particles. The formation of the solid shell around metallic particles is expressed as a function of the initial particle size and arc length.

Keywords: melting, DRI, metallic particles

Proces topnienia żelaza gąbczastego w piecu łukowym obejmuje wiele złożonych zjawisk związanych z przepływem cieczy, wymianą ciepła i masy w niestabilnych warunkach. Do tej poty kilkakrotnie próbowano powiązać te zjawiska, aby opisać proces kinetyki topnienia. W pracy przedstawiono wstępne rezultaty badań dotyczących tych trzech modeli; modelu łuku elektrycznego dla łuków prądu zmiennego, modelu kąpieli, modelu topnienia. Opisano również zależności pomiędzy zmianami w technologii procesu a kinetyką topnienia stałych cząstek. Tworzenie się stałej otoczki wokół metalicznych cząstek jest wyrażona jako funkcja początkowych rozmiarów cząstki i długości łuku.

1. Introduction

When a metallic particle is immersed in liquid steel the melting process initiates with the formation of a solid shell around those particles. Melting and dissolution of Direct Reduced Iron (DRI) particles is a complex phenomenon, affected by several factors, such as the thickness of the solid shell, magnitude of the convective heat transfer coefficient, DRI physical and chemical properties, etc. The first model on the melting of DRI in liquid silicate slags was reported by Elliot *et. al.*[1] in 1978. They evaluated the rate of melting of DRI under laboratory conditions and reported that by increasing both stirring conditions and slag temperature, the thickness of the frozen shell decreases. According with their model, a particle of 10 mm requires approximately 35 seconds to melt, this time is practically the same it takes to remelt the frozen shell. They also reported that small particles melt faster than large size particles with the exception of large particles with densities higher than that of the slag.

When DRI is continuously supplied into the Electric Arc Furnace (EAF), the first phase it encounters is the slag phase, a frozen shell of slag should then be formed around the particles, later on those particles are pushed inside the liquid steel and finally melted. DRI is a porous metallic material, which contains in addition to metallic iron, several oxides and carbon. In order to describe the thermal and chemical interaction of DRI with both slag and liquid steel it is necessary to know how the many process variables affect the melting and dissolution processes, however, there is a poor knowledge in this subject.

In this work, some preliminary results from a research work focused on the melting rate of metallic particles in liquid steel are reported, analyzing the influence of important process variables such as the initial particle size and electrical parameters associated with the power system in a three phase EAF of industrial scale.

* MORELIA TECHNOLOGICAL INSTITUTE. GRADUATE PROGRAM IN METALLURGY. AV. TECNOLÓGICO 1500, 58120 MORELIA, MÉXICO
** CHEMISTRY FACULTY. NATIONAL AUTONOMOUS UNIVERSITY OF MÉXICO

2. Mathematical Model

The mathematical model is limited to investigate the thermal interaction of DRI particles when placed in contact with liquid steel. It is composed of three sub-models; an arc model, a bath model and a melting model. A brief description of each sub-model is given below.

Arc Model

The arc model is required to compute the instantaneous electric power delivered by a three phase EAF. The electric power computed from the arc model for a given set of electrical parameters, such as voltage and arc length, is used as a boundary condition in the bath model.

There are two models available in the literature to characterize AC electric arcs. Both, the channel arc model (CAM) and the Magneto-Fluid-Dynamic Model (MFD) have been developed to study electric arc characteristics. MFD requires computational fluid dynamics software (CFD), in contrast, CAM not only can be solved in a regular personal computer but also the same results on the basic features of the electric arc can be computed. Therefore, CAM is used in the present investigation. This model is described in some detail by Larsen *et. al.* [1]. Air is assumed to form the plasma gas.

The bath and melting models can work decoupled from the arc model. The importance of having an arc model is in order to compute the instantaneous electric power available.

Bath Model

The bath model is required to describe fluid flow patterns due to thermal gradients. Body fitted coordinates (BFC) are used to represent the bath region. The thermal gradients will define the magnitude of both buoyancy forces as well as the heat transfer coefficient.

The governing equations describing fluid flow include the conservation of energy, the equation of continuity and the turbulent equations of Navier-Stokes.

In order to simplify the computations in this model, the following assumptions are made.

- Free surface
- Constant thermo-physical properties of liquid steel
- Walls at constant temperature of 1500°C
- Radiation from the walls and roof is not taken into account
- Steady state conditions in the flow

Governing equations

The governing equations correspond to the conservation of energy, momentum and mass; all of them can be represented by the following general expression, in rectangular coordinates.

$$\nabla \cdot \Gamma_\phi \nabla \phi - \nabla \cdot \left(\rho \overline{V} \phi\right) + S_\phi = \frac{\partial \rho \phi}{\partial t}, \tag{1}$$

Where:

ϕ = dependent variable, for example velocity and temperature.

Γ_ϕ = diffusion coefficient in $\mathrm{kgm^{-1}s^{-1}}$.

S_ϕ = source term(s) different to convective, diffusive or transient terms.

Boundary conditions:

Heat input: The heat flow generated by the 3-phase AC arcs is computed by the previous CAM model. For a given set of electric parameters (voltage and arc length), power delivery (P_0)represents a constant heat input, as indicated below.

$$-k_{eff} \frac{\partial T}{\partial z} = P_0, \tag{2}$$

Where: k_{eff} is the convective heat transfer coefficient.

Velocities: Non-slip boundary conditions, i.e. zero velocities, are imposed at the furnace walls. Zero shear stresses at the steel surface are possible by ignoring two driving forces; electromagnetic body forces and shear forces from the arc.

$$\begin{aligned} &\tau_{zy} = -\mu_{eff} \tfrac{dv_y}{dz} = 0; \quad @ -R \leqslant x \leqslant R; \\ &-R \leqslant y \leqslant R; z = H, \end{aligned} \tag{3}$$

Where: μ_{eff} represents the viscosity of the liquid, R the radius of the furnace and H the height of liquid steel.

Temperature at the walls is assumed to be constant, at 1500°C (1773°K).

The bath model reports velocity fields and temperature profiles in the entire computational domain.

Melting model

This model couples the bath model with the melting kinetics of solid particles, defining the melting rate of DRI pellets in the electric arc furnace as a function of several process variables.

In order to simplify the computations in this model, the following assumptions are made.

- Solid iron spheres of low density and uniform size are used to simulate DRI particles
- Liquid steel is the continuous phase and DRI particles represent the dispersed phase
- Uniform temperature in DRI particles

In order to simplify the model, the only source of thermal energy is due to the electric arc, neglecting the influence of exothermic chemical reactions.

The computational domain includes two phases; the dispersed phase (solids particles) and the continuous phase (liquid steel). The Lagrangian frame of reference was employed to track the movement of the solid particles.

The CFD code employed computes the movement and melting rate of each particle using the subroutine GENTRA (GENeral TRAcker). The movement is defined by Newtons's law of motion. The forces – buoyancy, dragging and added mass – acting upon each particle, are represented as follows:

$$\frac{dm_p U_p}{dt} = \frac{4}{3}\pi R_p^3 \left(\rho_p - \rho\right) g + 2\pi R_p^2 \\ C_D \rho \left|U_C - U_p\right| - C_A \frac{4}{3}\pi R_p^3 \rho \frac{dU_p}{dt}, \quad (4)$$

where: m_p is the mass the particle, U_p is the velocity of the particle, R_p is the radius of the particle, C_D is a drag coefficient between the fluid and the particle (its computation based on a correlation reported by Weber et. al.), g is the gravitational constant, ρ_p y ρ_l are the densities of both particle and fluid, respectively, and C_A a coefficient of added mass.

The equation which describes the temperature of the particle and its melting rate is the following:

$$Cp_p \cdot m_p \cdot \frac{\partial T_p}{\partial t} = m_p L_s \frac{df_s}{dt} + \alpha \left(T_c - T_p\right) \quad (5)$$

Where: Cp_p is the heat capacity of the particle, T_p and T_c are the temperatures of the particle and the liquid (continuous phase), respectively. L_s is the latent heat of melting, f_s is the solid fraction of each particle and α the heat transfer coefficient between the particle and the liquid. The solid fraction is computed based on data from the temperature of the particle, as follows.

$$f_s = \left(\frac{T_L - T_p}{T_L - T_S}\right)^m \quad (6)$$

Where f_s is the solid fraction, T_L is the particle liquidus temperature, T_S is the particle solidus temperature, T_p is the particle temperature, and m is a solidification index. Table 1 summarizes the thermophysical properties of solid DRI particles.

TABLE 1

Thermo-physical properties of DRI

Density, ρ_s	2500 kg/m^3
Thermal conductivity, k_P	0.58 W/kg °K
Heat capacity, C_P	627 J/kg °K
Heat of melting	274214 J/kg
Liquidus temperature	1768 °K
Solidus temperature	1708 °K

3. Results and analysis

The commercial CFD code PHOENICS vs.3.4 [2] was used to solve the complete set of partial differential equations, describing mass, energy and momentum conservation, using the technique volume of control (VOC).

The results reported in this work correspond to an industrial electric arc furnace of 220 ton of nominal capacity and the following general dimensions: extended top diameter 7.1 meters and bath depth of 1.53 m. **Figure 1** describes the computational domain.

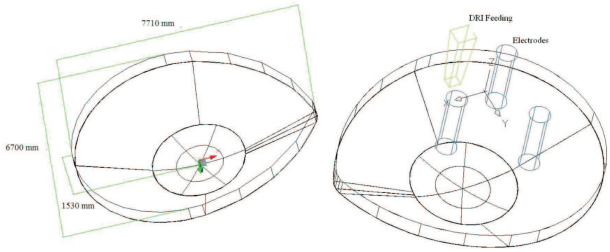

Fig. 1. Computational domain

Figure 2 describe some results from the channel arc model. This figure indicates the simultaneous effect of arc length and secondary voltage on the electric power produced by the three phase power system. It clearly shows that power delivery increases when arc length and voltage are increased. Operating at maximum tap of 1210 volts, power input will depend only on arc length. For an arc length of 25 cm the electric power produced is 90 MW, this is the case of a short arc operation. Operating with long arcs, such as 45 cm, the electric power increases up to 120 MW.

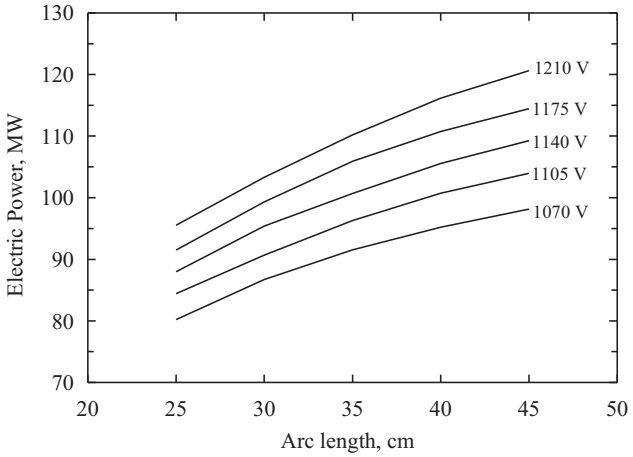

Fig. 2. Effect of arc length and arc voltage on power delivery

In the following simulations, the operation is carried out at a maximum voltage of 1210 volts. **Figure 3** shows the velocity fields for two conditions of arc length. The

only driving force acting upon the molten bath is due to buoyancy forces. Stirring due to oxygen injection and CO bubbling is not taken into account.

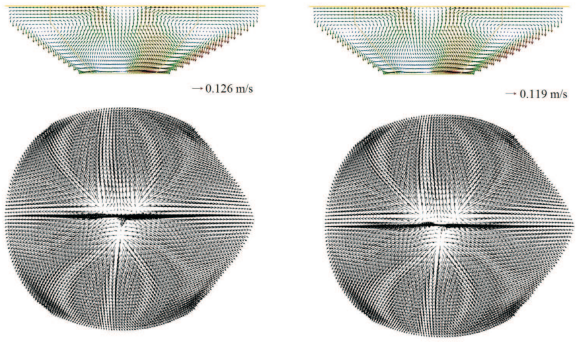

Fig. 3. Results from the bath model and two arc lengths. Left 45 cm and right 25 cm

In the previous figure, it can be observed the formation of two recirculatory loops which move upwards in the central axis. The maximum linear velocities are in the order of 0.12 ms^{-1}. This is a large value and is attributed to the high thermal input obtained with the highest voltage, in conjunction with the large thermal gradients in the vicinity of the walls where a low temperature was set as a boundary condition.

The poor stirring conditions in the Electric Arc Furnace can be expressed by considerable thermal gradients in the molten metal. **Figure 4** shows the temperature profile in the furnace. The difference between the hot and cold zones is in the order of 83°C. This thermal stratification is widely accepted as one of the limitations of EAF technology. The figure suggests a decrease in thermal stratification as arc length increases. Extremely high temperatures, in the order of 2650°C are concentrated in the region close to the electrodes.

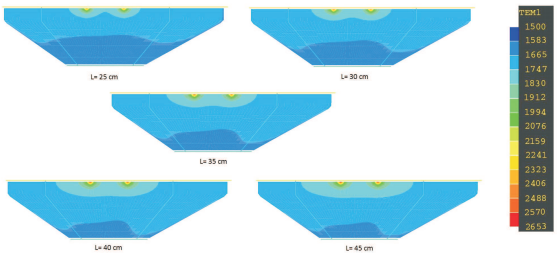

Fig. 4. Temperature profile as a function of arc length

The results on temperature profiles are influenced by the simplified boundary condition imposed to the walls. In a future work, this condition will be expressed in terms of heat fluxes.

In the following simulations the temperature of the solid particles is taken as 50°C. 500 solid particles are continuously fed by gravity which represent a flow rate of 3000 kg/min and a falling velocity of 8 ms^{-1}.

Figure 5 describes the growth of a frozen shell around DRI particles as soon as they came in contact with liquid steel. The particle size increases by about 41%, independently of arc length, in other words, independent of the heat input. However, by increasing arc length the overall melting time decreases. The model predicts a melting time of approximately 13 seconds for an initial particle size of 12 mm. The thickness of the solid shell is approximately 5 mm and it takes about 6 seconds to be re-melted. The overall melting time is small; this is due to the large thermal conductivity of steel that forms the shell and thus explains the differences with the melting model in slags reported by Elliot *et al.* [1]. The simulated DRI particles behave as high melting point ferroalloys. In this case, the particle melts after the melting of the frozen shell.

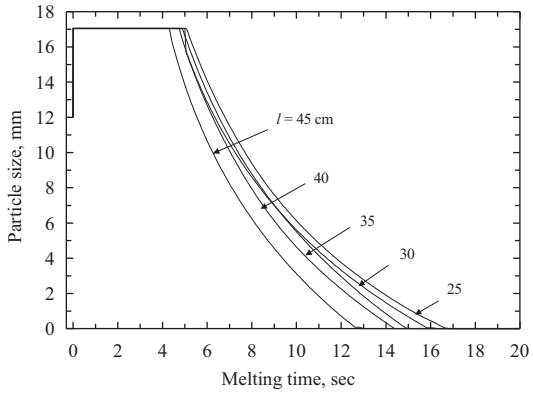

Fig. 5. Frozen shell formation and melting rate

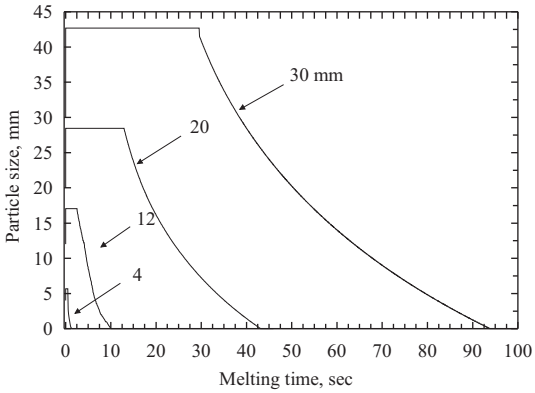

Fig. 6. Melting rate as a function of the initial particle size

Figure 6 shows the growth of the frozen shell for various particles of different initial particle size and for an arc length of 45 cm. It is shown that as the initial particle size increases, also increases the thickness of the frozen shell, consequently the melting rate will decrease. The time to re-melt the frozen shell changes with the initial particle size. Longer particles will require longer re-melting times. This result is in agreement with

those of Elliot *et al.* [1], however, it can be misleading. Small particles do not have the momentum required to penetrate the liquid phase and will end up on the surface. In these circumstances they will never melt.

Figure 7 shows in more detail the melting kinetics of one particle of 10 mm. According to Elliot a particle of 10 mm requires 35 seconds to melt. Our results indicate a melting time of only 12 seconds. This difference is easily explained due to the much higher thermal conductivity of steel in comparison with that of the slags, furthermore, it is also observed that the melting time to remelt the frozen shell is smaller in comparison with the time it takes to melt the core of the particle, this can be explained in terms of the different masses involved.

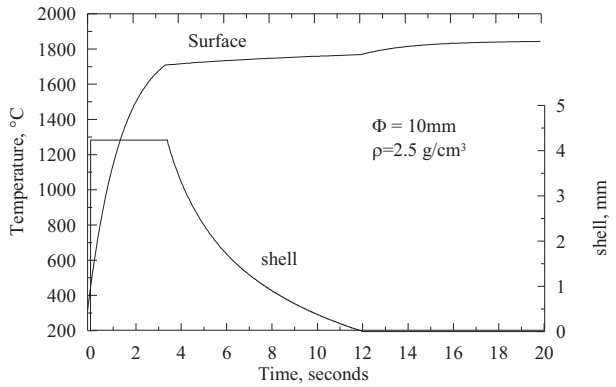

Fig. 7. Melting rate as a function of the initial particle size

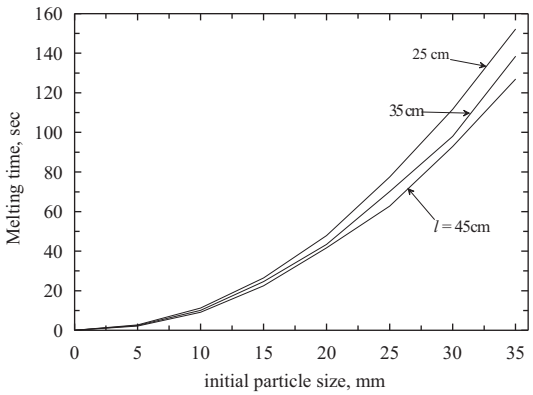

Fig. 8. Melting rate as a function of arc length

One important feature of this investigation refers to the key role played by the electrical parameters on the melting kinetics of metallic particles. **Figure 8** shows the influence of arc length on melting time for particles of different initial size. For particles below 10 mm, arc length plays a minor role, however, when the initial particle size is above 20 mm, an increment in arc length drastically decreases the melting time. In practice there is a large variation in particle size, however, good DRI ranges from 10-16 mm. **Figure 9** shows more clearly the influence of arc length on the melting rate, for particles of 12 mm. A comparison from short arc operation to large arc operation decreases the melting time by 3 seconds in each particle.

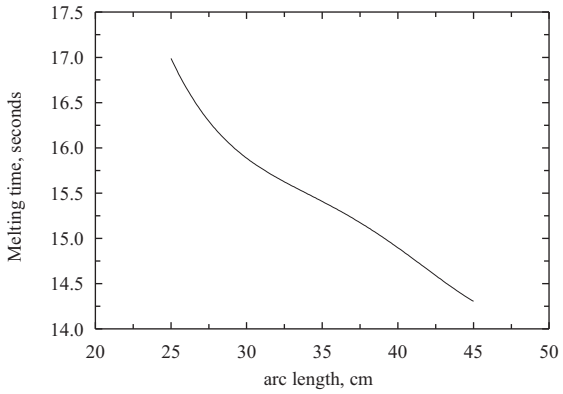

Fig. 9. Melting rate as a function of arc length

An important aspect in DRI melting operations is the location of the feeding chute. Ideally, this chute should be placed as close as possible to the hottest zone in the furnace. **Figure 10** shows the influence of different feeding positions. It is evident from this results that the ideal location is exactly in the central part of the pitch circle (position 2). This is the hottest zone in the furnace, however it appears that there are practical limitation to supply DRI in this position. It is more common to introduce DRI in position 1, in this position there is an increase in melting time but the change is smaller in comparison with other feeding positions.

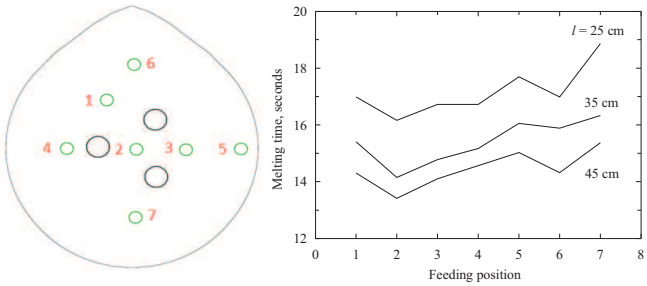

Fig. 10. Melting rate as a function of feeding position in the EAF

Another aspect in DRI melting is the initial temperature. Current technologies promote the feeding of hot DRI, using special transport from the reduction furnaces when the reduction plants are located close to the steelshops or by placing small reduction plants above the EAF. The central idea is to decrease energy requirements and decrease the melting time. **Figure 11** shows the model predictions in regard to the initial temperature of the solid particle of 12 mm. Operating with long arcs, for example 45 cm, there is a decrease in melting time of more than 1 second per particle when the temperature is increased from room temperature to 500°C.

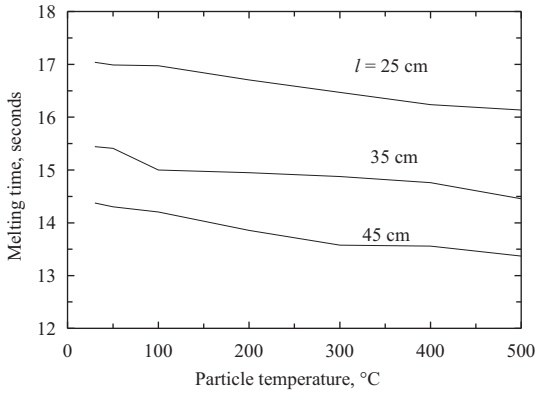

Fig. 11. Melting rate as a function of arc length

4. Conclusion

The melting rate of the simulated DRI particles in liquid steel was analyzed by mathematical modeling. The preliminary results suggest a strong influence of the initial particle size and arc length. In order to decrease the melting time it is convenient to operate with long arcs, with smaller size particles, hot charging and a feeding position as close as possible to the hottest zone in the furnace.

The formation and melting of the solid shell around the solid particles plays a big role in the overall melting kinetics. The thickness of this shell was found independent of the heat input but directly related to the initial particle size.

The model also indicates a strong thermal stratification in the Electric Arc Furnace, however, with a long arc operation this problem can be decreased.

Received: 2 April 2008.

REFERENCES

[1] J. F. Elliot, J. Nauman, K. Sadrnezhaad, Proc. Third Int. Iron and Steel Congress, ASM-AIME, Chicago Ill, USA, April 16-20, 397-404 (1978).
[2] H. L. Larsen, G. A. Sœvarsdottir, J. A. Bakken, 54^{th} Electric Furnace Conference Proceedings, Dallas TX, USA, 9-12 Dec., 157-168 (1996).
[3] PHOENICS^{TM} Software, v.3.4, CHAM Ltd., London U.K., June 2001.